Sre1, an Iron-Modulated GATA DNA-Binding Protein of Iron-Uptake Genes in the Fungal Pathogen *Histoplasma capsulatum*†

Lily Y. Chao,‡ Michael A. Marletta,*,§,||,⊥ and Jasper Rine*,§,⊥

Department of Molecular and Cell Biology, Department of Chemistry, Department of Plant and Microbial Biology, California Institute for Quantitative Biosciences, and Division of Physical Biosciences, Lawrence Berkeley National Laboratory, University of California, Berkeley, California 94720-3220

Received January 12, 2008; Revised Manuscript Received March 18, 2008

ABSTRACT: The pathogenic fungus *Histoplasma capsulatum* requires iron for its survival during macrophage infection. Because iron is toxic at high levels, iron acquisition in pathogenic organisms, including *H. capsulatum*, is a highly regulated process. In response to excess iron, *H. capsulatum* represses transcription of genes involved in iron uptake. We report here that *SRE1*, a gene encoding a GATA-type protein, bound to promoter sequences of genes involved in siderophore biosynthesis. Sre1 had sequence similarity to the fungal negative regulators of siderophore biosynthesis. Expression of *SRE1* was reduced under iron-starving conditions, underscoring its role as a negative regulator of genes involved in iron uptake. Sre1p specifically bound DNA containing the 5′-(G/A)ATC(T/A)GATAA-3′ sequence, and that binding was both iron- and zinc-dependent. Metal analysis indicated that a substoichiometric amount of iron, predominately Fe^{3+}, was bound to the purified protein. About 0.5−1 equiv of Fe^{3+} per monomer was necessary for full DNA-binding activity. Mutations in the conserved cysteine residues in the cysteine-rich region led to a decrease in bound iron. The loss of iron led to a ∼2.5-fold decrease in DNA-binding affinity, indicating that iron was directly involved in *SRE1* regulation of iron-uptake genes.

Histoplasma capsulatum is a pathogenic dimorphic fungus that causes respiratory and systemic mycosis, especially in immunocompromised individuals (*1*). *H. capsulatum* exists in two morphological forms: a mycelial form in soil and a budding yeast form in the host. Infection occurs when spores are inhaled into the lungs, where the organism converts into the budding yeast form. *H. capsulatum* is ingested by macrophages and multiplies within the phagolysosome of the macrophage. *Histoplasma* may persist in the lung for decades in a latent state, or it can disseminate widely in the body, particularly the liver, spleen, and bone marrow, leading to systemic infection and potentially death.

Similar to most microorganisms, *H. capsulatum* requires iron for growth. Iron is an essential cofactor in key metabolic processes ranging from respiration and nucleic acid synthesis (*2*). Its sequestration inhibits *H. capsulatum* growth *in vitro* and in macrophages (*3–5*). Although iron is the second most abundant metal on Earth, in aerobic environments, free iron is present in insoluble compounds, such as ferric hydroxides. During infection, most of the iron of the host is present in iron-binding proteins, such as transferrin, lactoferrin, hemoglobin, heme, and hemin (*6–8*). However, an excess of iron is toxic because it catalyzes the production of cell-damaging free radicals (*9, 10*). Therefore, iron acquisition is an essential function that is a tightly regulated process. In pathogens, the lack of iron also serves as an environmental signal that leads to the expression of virulence factors, such as toxins that cause the release of iron from the host, as well as activating genes involved in iron uptake (*11, 12*). The same regulators that control iron-acquisition mechanisms often regulate expression of these virulence factors.

To obtain iron from the host or the environment, most bacteria and fungi synthesize and secrete low-molecular-weight compounds called siderophores, which chelate ferric iron with high specificity and affinity. With the exception of the Zygomycetes, which produce carboxylate-type siderophores, most fungi, including *H. capsulatum*, produce and secrete hydroxamate-type siderophores under low iron-growth conditions (*13, 14*).

The regulation of siderophore biosynthesis and its effect on bacterial pathogenicity is well-established (*15–17*). However, there is less information on the molecular basis of iron acquisition in fungi and its impact on fungal pathogenesis. The mechanism and regulation of iron acquisition in the yeast *Saccharomyces cerevisiae* is relatively well-understood. However, *S. cerevisiae* differs from most fungi, in that it does not synthesize and secrete its own siderophores but, instead, can take up iron-bound siderophores secreted by other fungi (*18*).

† Funding was provided by grants from the National Institutes of Health (NIH) (GM31105 and GM35827 to J.R.).

* To whom correspondence should be addressed: California Institute for Quantitative Biosciences, University of California—Berkeley, 570 Stanley Hall, Berkeley, CA 94720-3220. Telephone: (510) 666-2766. Fax: (510) 666-2765. E-mail: marletta@berkeley.edu (M.A.M.); California Institute for Quantitative Biosciences, University of California—Berkeley, 392 Stanley Hall, Berkeley, CA 94720-3220. Telephone: (510) 642-7047. Fax: (510) 666-2768. E-mail: jrine@berkeley.edu (J.R.).

‡ Department of Plant and Microbial Biology.

§ Department of Molecular and Cell Biology.

|| Division of Physical Biosciences, Lawrence Berkeley National Laboratory.

⊥ California Institute of Quantitative Biosciences.

10.1021/bi800066s CCC: $40.75
Published on Web 06/13/2008

Thus far, all fungi that produce their own siderophores encode a protein that is a member of the GATA family of transcriptional regulators and acts as a negative regulator of siderophore biosynthesis and use under iron-replete conditions. GATA proteins are present in plants, fungi, and metazoans and regulate many metabolic processes, such as terminal differentiation and nitrogen metabolism (*19–21*). Their consensus recognition motif is a six base-pair sequence, HGATAR (H = T or A, and R = A or G) (*20, 21*). Urbs1 from the Basidiomycete *Ustilago maydis* was the first fungal GATA factor involved in regulation of siderophore biosynthesis to be identified and characterized. Homologous GATA factors that also regulate siderophore production were identified in the Ascomycetes *Neurospora crassa* (SRE), *Penicillium chrysogenum* (SREP), and *Aspergillus nidulans* (SREA) and in *Schizosaccharomyces pombe* (Fep1p) (*22–25*). The classic GATA DNA-binding domain is comprised of a Cys_2/Cys_2-type zinc finger, and the fungal GATA factors that regulate iron metabolism all contain two typical GATA-type zinc finger DNA-binding domains, whereas the others will have single DNA-binding domains. In addition to the zinc finger domains, there is a highly conserved region found between the zinc fingers, called the cysteine-rich region (CRR),[1] which is important for iron sensing (*24, 26–28*). However, there has been no evidence showing that these proteins directly bind iron.

The *U. maydis* Urbs1 protein represses the expression of *sid1*, which encodes L-ornithine-N^5-oxygenase, the enzyme that catalyzes the first committed step of siderophore biosynthesis, by directly binding to GATA motifs in the *sid1* promoter (*29*). Interestingly, the *SID1* homologue in *H. capsulatum* was recently identified by Hwang et al. (*42*) as one of a group of six siderophore biosynthesis genes whose expression is induced by iron limitation. Hwang et al. identified a consensus site [5′-(G/A)ATC(T/A)GATAA-3′] that is present at least once in the promoters of all of these genes, suggesting that the site may contribute to the regulation of gene expression by a *H. capsulatum* GATA factor in response to iron levels.

In this study, we identified the *H. capsulatum* GATA-type negative regulator of siderophore biosynthesis, Sre1p. We examined its DNA-binding characteristics by gel electrophoretic-mobility-shift assays (GEMSAs) using probes that contained the consensus sequence 5′-(G/A)ATC(T/A)GATAA-3′. Furthermore, we quantified the iron and zinc content of the protein by inductively coupled plasma atomic emission spectroscopy (ICP-AES) and examined their contribution to DNA binding. These results, together with data on other characterized GATA-type iron regulators, were used to address how iron uptake is regulated in fungi.

[1] Abbreviations: IPTG, isopropyl-β-D-thiogalactopyranoside; HEPES, 4-(2-hydroxyethyl)piperazine-1-ethanesulfonic acid; SDS−PAGE, sodium dodecyl sulfate−polyacrylamide gel electrophoresis; EDTA, ethylenediaminetetraacetic acid; BME, β-mercaptoethanol; poly(dI−dC), poly(deoxyinosinic−deoxycytidylic) acid; MBP, maltose-binding protein; GZF, GATA-type zinc finger; CRR, cysteine-rich region; BPS, bathophenanthroline disulfonic acid; ICP−AES, inductively coupled plasma atomic emission spectroscopy; GEMSA, gel electrophoretic-mobility-shift assay; Sre1p, siderophore uptake regulator protein.

MATERIALS AND METHODS

Strains and Culture Conditions. Stock cultures of *H. capsulatum* strain G217B were grown in histoplasma macrophage medium (HMM), which contains 3 μM $FeSO_4$ (*30*). RNA samples acquired for quantitative reverse transcription-polymerase chain reaction (qRT-PCR) analysis were isolated from cultures grown in 500 mL of HMM to early logarithmic phase. Three aliquots of cells representing untreated 0 h time points were harvested. The remaining cells were split into six 75 mL cultures, with half supplemented with 10 μM ferric citrate and the other half supplemented with 100 μM deferoxamine mesylate (Sigma), representing iron-replete or iron-starved conditions, respectively. Samples were harvested after 1, 4, and 12 h for RNA isolation.

Expression and Purification of MBP−His_6−Fusion Protein. The pETMALc-H vector was used to express Sre1p (residues 116−374) and its different mutant forms as fusion proteins with both the maltose-binding protein (MBP) and a His_6 tag (*31*). The cDNA fragment encoding Sre1p (116−374) along with a stop codon was cloned in-frame with the MBP−His_6 tag fused to the amino terminus of Sre1p. All site-directed mutations in *SRE1* were generated using QuikChange site-directed mutagenesis (Stratagene). The sequence changes were confirmed by DNA sequencing.

The pETMALc-H/Sre1p (116−374) plasmid was transformed into *Escherichia coli* Rosetta 2(DE3) cells (Novagen) for protein expression. A single colony was used to inoculate 5 mL of LB medium containing 50 μg/mL kanamycin and then grown with shaking at 37 °C. After overnight growth, 600 mL of fresh medium was inoculated with the overnight culture. The culture was grown at 250 rpm at 37 °C to an OD_{600} of ∼0.6. Expression of MBP−His_6−Sre1p was then induced by the addition of 0.5 mM isopropyl-β-D-thiogalactopyranoside (IPTG). The culture was shaken for another 4 h before the cells were harvested by centrifugation and stored at −80 °C.

Ni-affinity chromatography was used for protein purification. Frozen pellets were thawed and suspended in buffer A [25 mL of 50 mM Na_2HPO_4 (pH 7.5), 300 mM NaCl, 20 mM imidazole, 5 mM β-mercaptoethanol (BME), and 5% glycerol]. The cell suspensions were then lysed with an Emulsiflex-C5 high-pressure homogenizer (Avestin, Inc.) and pelleted at 140000*g* for 15 min. After centrifugation, the supernatant was applied to a 1.5 mL column of Ni−NTA Superflow resin (Qiagen) equilibrated with buffer A. The column was washed with five column volumes of buffer A and one column volume of buffer A containing 1 M NaCl. Bound protein was eluted with 250 mM imidazole in buffer A. The eluted protein was concentrated to <1 mL using a Vivaspin-6 50K filter (Vivascience) before it was buffer-exchanged with 20 mM 4-(2-hydroxyethyl)piperazine-1-ethanesulfonic acid (HEPES) (pH 7.5), 100 mM NaCl, 5 mM dithiothreitol (DTT), and 5% glycerol using a PD-10 column (GE Healthcare) and stored at −80 °C.

Analytical Gel Filtration of Purified Protein. MBP−His_6−Sre1p was further purified by gel filtration on a Superdex S75 Hiload 16/60 column (Pharmacia) before analytical gel filtration analysis. Analytical gel filtration on MBP−His_6−Sre1p was performed on a Hewlett-Packard 1090 liquid chromatograph equipped with a ZORBAX Bio Series GF-250 gel filtration column (Agilent). The column

Table 1: Summary of Apparent K_d Values[a]

construct	probe	K_d (nM)
wild type	*SID3(−575)*	90
wild type	*ABC1(−317)*	147
Zn^{2+} reconstituted[b]	*SID3(−575)*	230
crr1	*SID3(−575)*	250
crr2	*SID3(−575)*	205
crr1−crr2	*SID3(−575)*	227

[a] Apparent K_d values were calculated using densitometry and fitting data to eq 1. [b] Zn^{2+} reconstituted was prepared by dialyzing EDTA-treated wild-type Sre1p against 5-fold excess $ZnCl_2$.

was run in 200 mM potassium phosphate (pH 7.4) and 150 mM NaCl. The standards used were cytochrome *c* (12.4 kD), ovalbumin (45 kD), bovine serum albumin (66 kD), yeast alcohol dehydrogenase (150 kD), and thyroglobulin (669 kD) (Sigma). Sample concentrations were 2 μg/uL upon loading. All proteins were detected by absorbance at 280 nm.

Gel Electrophoretic-Mobility-Shift Assays (GEMSAs). Complementary synthetic oligonucleotides (Integrated DNA Technologies) were annealed and 5′-end-labeled using [γ-^{32}P]ATP (Perkin-Elmer) and T4 polynucleotide kinase (NEB). The unincorporated [γ-^{32}P]ATP was removed using a Micro Bio-Spin 6 column (BioRad), and the amount of radioactivity was measured by scintillation counting.

GEMSAs were carried out in 12 mM HEPES, 4 mM Tris-HCl (pH 7.5), 150 mM KCl, 2.5 mM BME, 5% glycerol, and 1 μg of poly(deoxyinosinic−deoxycytidylic) acid [poly(dI−dC)]. Varying amounts of MBP−His_6−Sre1p (0−1 μg) were incubated with 20 000 cpm of labeled probe at room temperature for 25−30 min and then loaded on a 5% native polyacrylamide gel (29:1 acrylamide/bis ratio) that had been prerun in 0.25× TBE for 30 min. The DNA−protein complexes were separated from free probe by electrophoresis for 1 h and 40 min at 150 V. The gel was dried, exposed to a PhosphorImager screen (GE Healthcare), and scanned on a Typhoon Imager (GE Healthcare). Apparent K_d values for the probes that yielded single shifts were determined using band densitometry. Band intensity measurements were carried out using ImageQuant version 5.2 (Molecular Dynamics). The log [protein concentration] versus the ratio [bound probe/free probe] plot was fitted to a four-parameter sigmoidal dose−response curve (eq 1) to determine the apparent probe-binding dissociation constants, where m_0 = log[protein concentration], m_1 = minimum bound/free probe, m_2 = maximum bound/free probe, m_3 = Hill coefficient, and m_4 = apparent K_d using Kaleidagraph version 4.01 (Synergy) (*32, 33*). The apparent K_d values are summarized in Table 1.

$$\text{bound/free} = m_1 + \frac{(m_2 - m_1)}{(1 + 10^{(-m_3(m_0 - \log(m_4)))})} \quad (1)$$

Zinc and Iron Determination of Purified Protein. The amount of zinc and iron metal in purified MBP−His_6−Sre1p and its mutants were determined by ICP-AES. All protein samples and metal standards (SPEXCertiPrep Group) were diluted in 1% trace-metal-grade HCl (Fisher Scientific). All solutions were made with metal-free water and prepared in plasticware to avoid trace-metal contamination. Protein samples were prepared in tri- or quadruplicate and analyzed on an Optima 3000DV (Perkin-Elmer).

Quantitative PCR. Total RNA was purified from *H. capsulatum* using Trizol reagent (Invitrogen). Cells were lysed in Trizol by vortexing in the presence of glass beads, and total RNA was isolated according to the recommendations of the manufacturer. DNA was digested with RNase-free DNaseI (Fermentas). cDNA was synthesized using the Thermoscript RT-PCR system and oligo-dT (Invitrogen). Quantitative analyses of *SRE1* and *ACT1* were carried out with a SYBR Green PCR mix and incubated in an Mx3000P qPCR system (Stratagene). The primers used for *SRE1* amplification were forward primer, 5′-AATGATGGGAAT-GATCCTCGGCTG-3′, and reverse primer, 5′-CGTTCT-CGGAGTATGGAGCG-3′. The primers used for ACT1 amplification were forward primer, 5′-TCCGAAAGGATC-TCTACGGCAACA-3′, and reverse primer, 5′-TCCA-CATTTGCTGGAAGGTCGAGA-3′. Samples were analyzed in triplicate.

Determination of the Iron Oxidation State in MBP−His_6−Sre1p. The oxidation state of the iron in Sre1p was determined by the bathophenanthroline disulfonic acid (BPS) assay (*34*). BPS dye was added to Sre1p with and without the addition of dithionite. The absorbance of the Fe^{2+}−BPS complex was measured at 535 nm.

Metal Removal and Zinc Reconstitution. Zn^{2+}-reconstituted Sre1p was prepared in the following way: purified Sre1p was dialyzed overnight against buffer containing 20 mM HEPES (pH 7.5), 100 mM NaCl, 100 mM ethylenediaminetetraacetic acid (EDTA), and 5% glycerol. EDTA was removed by dialysis against buffer without EDTA. For Zn^{2+} incorporation, metal-free protein was dialyzed against 5−10 equiv of $ZnSO_4$. Excess metal was removed by dialysis against HEPES buffer with no metal. The amount of Zn^{2+} incorporated was determined by ICP-AES.

RESULTS

Identification of SRE1. A BLAST search using *A. nidulans* SREA amino acid sequence as the query against the *H. capsulatum* G217B genome database yielded a genomic DNA sequence that, upon conceptual translation, had a region with significant similarity to the GATA zinc finger motif (Figure 1). The full-length cDNA sequence (GenBank accession number bankit1026083 EU220030) containing the *SRE1* open-reading frame was identified by 5′ and 3′ rapid amplification of cDNA ends (RLM-RACE, Ambion). Comparisons of the genomic DNA and cDNA sequences showed that the open-reading frame was interrupted by two introns, each located within the zinc finger domains. The location of these introns is conserved among the iron-regulating GATA factors in Ascomycetes (*22, 23, 35*).

The Sre1 protein had a calculated mass of 67.3 kDa and the highest overall sequence similarity to the iron-regulating GATA transcription factors of *A. nidulans* SREA (46.3% identity) and *N. crassa* SRE (35.2% identity). A multiple sequence alignment showed that Sre1p had two GATA-type zinc finger domains (GZF1 and GZF2) (*21*). Additionally, there was a region of significant sequence similarity between the two zinc finger domains. This region of additional similarity had four conserved cysteine residues and, hence, has been referred to as the CRR. Similar to SREA and SRE, Sre1p also contained a conserved C-terminal domain, which may mediate protein−protein interactions (*23*).

Purification of MBP−His_6−Sre1p(116−374). A 259 amino acid fragment containing the GATA-type zinc finger domains

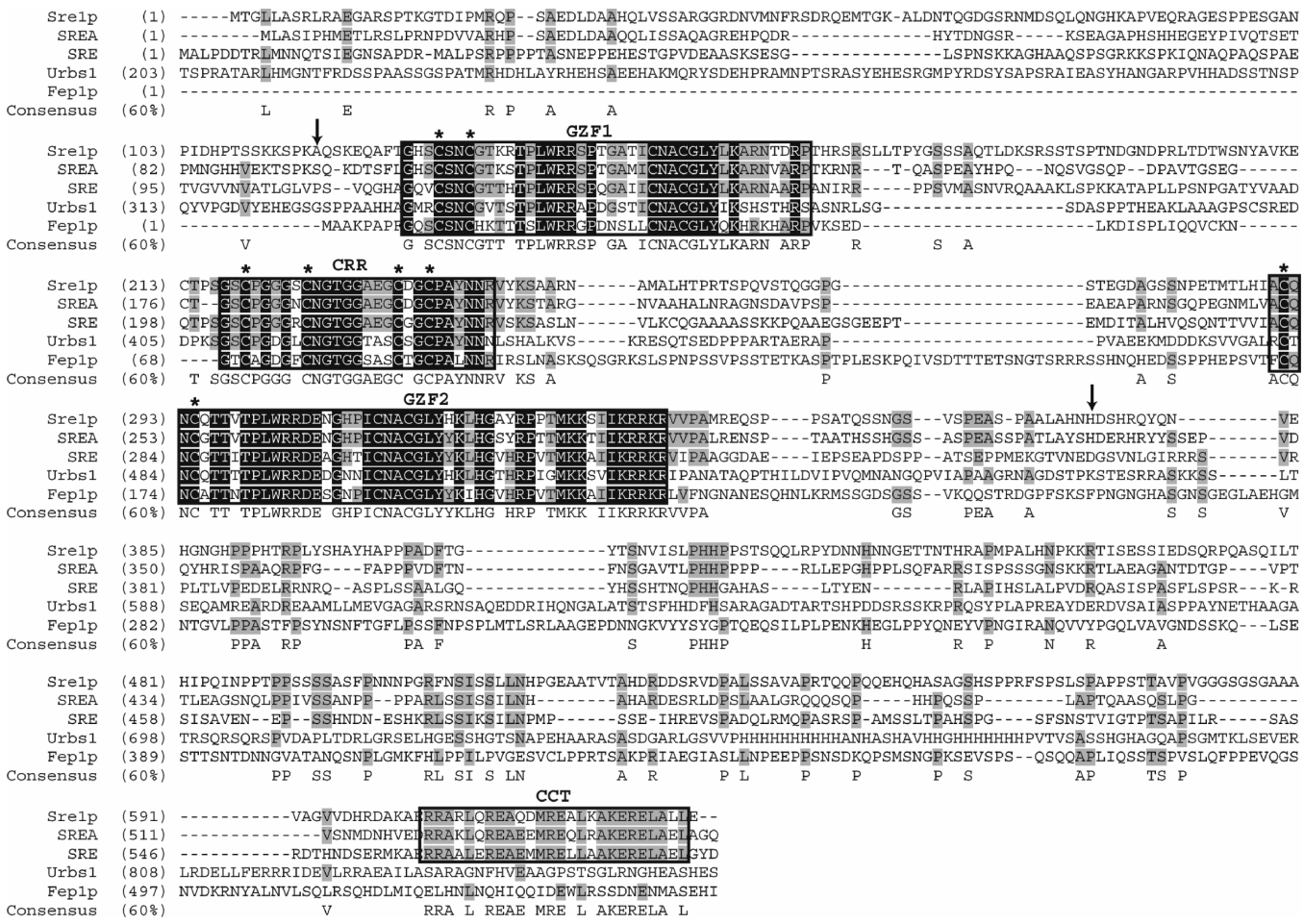

FIGURE 1: Alignment of *H. capsulatum* Sre1p, *A. nidulans* SREA, *N. crassa* SRE, *U. maydis* URBS1, and *S. pombe* Fep1p. Identical amino acids are shaded in black. Residues that match the consensus are shaded in gray. The GATA-type zinc fingers (GZF1 and GZF2), the cysteine-rich region (CRR), and the conserved C terminus (CCT) are boxed. Mutations made in this study are marked (∗). The arrows denote the region of the protein that was purified. The alignments were generated using AlignX from Vector NTI (Invitrogen).

and the cysteine-rich region was expressed and purified with a N-terminal MBP−His_6 tag. The MBP tag allowed for high-yield expression of soluble protein, whereas the His_6 tag allowed for purification by nickel-affinity chromatography. Both wild-type and mutant constructs made in this study were purified to >90% homogeneity as assessed by sodium dodecyl sulfate−polyacrylamide gel electrophoresis (SDS−PAGE) (Figure 2A). The contaminating proteins were likely degradation products of the expressed protein and were mostly removed by gel filtration.

During nickel-affinity purification, the wild-type and zinc finger mutants eluted as an orange−brown-colored protein, suggesting that Fe^{3+} was bound to the protein. However, this orange−brown color disappeared after a few hours if the protein was left in reducing buffer conditions at 4 °C and not immediately frozen. This change in color was also observed when a strong reducing reagent, such as dithionite, was added to the freshly purified protein. In contrast, the cysteine-rich mutants eluted as yellow-colored protein, suggesting that either there was no longer any iron bound to the protein or that the iron was reduced. Analogous observations have been described for SRE from *N. crassa* (*26*).

Purified wild-type Sre1p [MBP−His_6−Sre1p(116−374)] with a predicted molecular weight of 70 kDa, ran predominantly as a monomer at 69 kDa when subjected to analytical gel filtration (Figure 2B). A small shoulder was observed at 111 kDa, which may reflect a small amount of dimeric protein. All of the mutant proteins eluted similarly to that of the wild type.

DNA Binding of Sre1p. The ability of wild-type Sre1p(116−374) to bind to the consensus GATA motif identified by Hwang et al. was assessed by GEMSA using double-stranded DNA probes containing the conserved GATA motif from the promoters of the iron-responsive genes *SID3* (an acetylase) and *ABC1* [an ATP-binding cassette (ABC) transporter] (*42*) (Figures 3A and 4A). The *SID3* and *ABC1* promoters both contained several copies of the GATA motif. Two copies from each promoter were used: *SID3(−431)* and *SID3(−575)* and *ABC1(−496)* and *ABC1(−312)*; the numbers represent the location upstream of the start codon (+1). A single-shifted band was observed when *SID3(−575)* and *ABC1(−317)* were used as probes (Figure 3B). There was also a faint second shifted band at 250−500 nM Sre1p. Sre1p bound to *SID3(−575)* and *ABC1(−317)* with an apparent K_d of 90 and 147 nM, respectively (Table 1). Double-shifted bands were observed with the *SID3(−431)* and *ABC1(−496)* probes (Figure 4B). The second shifted band was evident between 100−150 nM Sre1p for *SID3(−431)* and 250−500 nM Sre1p for *ABC1(−496)*. The second shifts may have resulted from dimerized Sre1p.

Mutations in the GATA motif of the *SID3(−575)* probe indicated that the shift was GATA-dependent (Figure 3C).

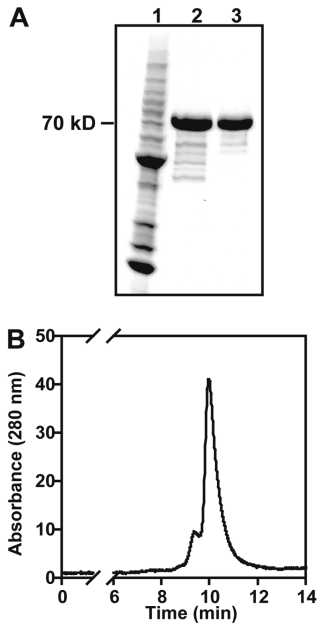

FIGURE 2: Gel filtration of Sre1p [MBP−His_6−Sre1p(116−374)]. (A) SDS−PAGE gel analysis of Sre1p. Lane 1, Benchmark molecular-weight marker; lane 2, Sre1p (~3 μg) after Ni-affinity purification; lane 3, Sre1p after gel filtration. (B) Analytical gel filtration of Sre1p. The standards used were cytochrome *c* (12.4 kDa, 11.8 min), ovalbumin (45 kDa, 10.4 min), bovine serum albumin (66 kDa, 9.7 min), yeast alcohol dehydrogenase (150 kDa, 9.3 min), and thyroglobulin (669 kDa, 7.8 min). The standards were plotted as the log of the molecular weight versus retention time, and the data were fitted to a linear line, which had a slope of 2.287, a *y* intercept of 21.04, and a R^2 of 0.986. There was one main Sre1p peak at 10 min and a small shoulder at 9.5 min. On the basis of these retention times and a predicted molecular weight of 70 kDa, Sre1p was mostly a monomer with a native molecular weight of 69 kDa.

Only at high concentrations (0.25−0.5 nM) of Sre1p(116−374) was a small amount of the *SID3(−575)* mutant GATA site probe shifted. The shift was abolished when the entire consensus element was replaced with a randomly permuted sequence.

To further examine the DNA-binding specificity of Sre1p(116−374), a 65 bp DNA fragment of the *SID1* promoter that included two GATA sequences, *SID1(−684)*, was used for GEMSA. Transcription of *SID1*, which encodes L-ornithine-N^5-oxygenase, is negatively regulated by iron (*42*). *SID1(−684)* contained two GATA motifs similar to the consensus, which occur within 4 bp of each other on opposite strands (Figure 4C). GEMSA indicated that Sre1p bound to the *SID1(−684)*. Up to three-shifted probe complexes were observed, with the higher two shifts being predominant at higher protein concentrations (360−720 nM). This band-shift trend was similar to that observed with *N. crassa* SRE and the *U. maydis sid1* iron-response element (*26*). Further gel-shift analyses showed that Sre1p bound specifically to the GATA elements but not to the flanking sequence (Figure 4C).

Metal Analysis of Purified Protein. The zinc and iron content of wild-type and mutant Sre1p(116−374) was analyzed by ICP-AES. As isolated, wild-type Sre1p contained approximately 1.6 equiv of zinc per monomer, a value close to the predicted 2 equiv of zinc expected for the two GATA-type zinc finger domains (Table 2). In contrast, most of the mutants examined in this study contained less zinc than the

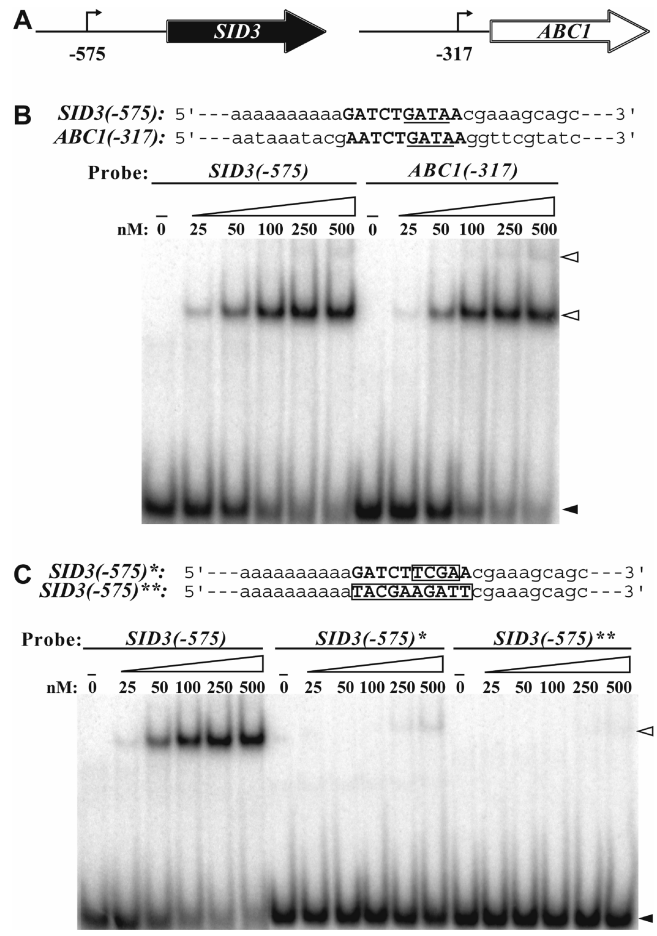

FIGURE 3: DNA binding of Sre1p. (A) Consensus GATA elements upstream of the iron-regulated genes *ABC1* and *SID3*. The 52 bp [*ABC1(−317)* and *SID3(−575)*] probes containing these GATA elements (positions indicated by arrows) were used for mobility shift analysis. (B) Sre1p bound to ^{32}P-labeled *ABC1(−317)* and *SID3(−575)* probes with an increasing amount (0−500 nM) of protein. The sequences for *ABC1(−317)* and *SID3(−575)* are shown in the top panel with the consensus sequence in bold and the GATA motif underlined. (C) Sre1p bound *SID3(−575)* but not *SID3(−575)**, in which the GATA element was mutated, and *SID3(−575)***, in which the consensus sequence was randomized. The sequences for *SID3(−575)** and *SID3(−575)*** are shown with the consensus sequence in bold and the mutated sequence boxed. The black arrow indicates the unbound probe, and the white arrows indicate the shifted species.

wild-type protein. Mutations in either GATA zinc finger domain lead to a decrease in approximately 1 equiv of zinc in Sre1p: gzf1 (C128A/C131A) contained 0.7 equiv of zinc and gzf2 (C291A/C294A) contained 0.94 equiv of zinc. Interestingly, even when both zinc finger domains are mutated, the double zinc finger domain mutant, gzf1−gzf2 (C128A/C131A/C291A/C294A), still contained 0.6 equiv of zinc. The CRR mutants, crr1 (C219A/C225A), crr2 (C234/C237A), and crr1−crr2 (C219A/C225A/C234A/C237A), contained ~1.3 equival of zinc, which was within error of the amount measured in wild-type Sre1p.

Iron content analysis revealed that purified Sre1p contained substoichiometric amounts of iron. The wild-type protein contained the most, ~0.5 equiv per monomer, whereas all of the CRR mutants contained <0.25 equiv. The quadruple cysteine mutant, crr1−crr2, contained the least amount of iron at 0.06 equiv, approximately half the amount compared to when two cysteine residues are mutated (crr1 and crr2).

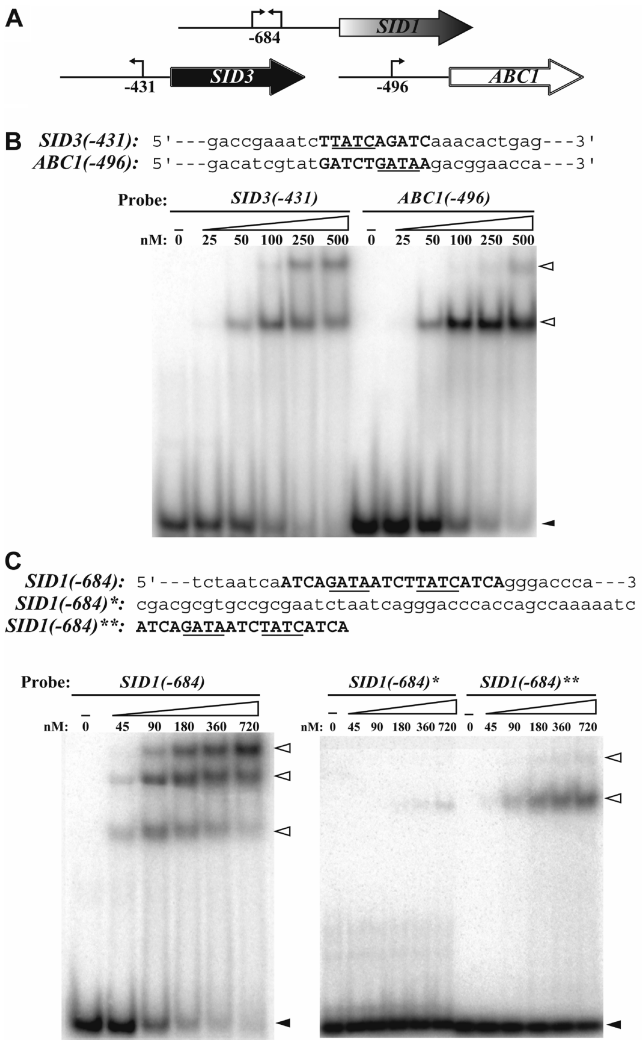

FIGURE 4: Other consensus GATA sequences bound by Sre1p. (A) Consensus GATA elements upstream of the iron-regulated genes *ABC1*, *SID1*, and *SID3*. The 64 bp [*ABC1(−496)* and *SID3(−431)*] and 65 bp [*SID1(−684)*] probes containing these GATA elements were used for GEMSA. (B) GEMSA result with probes *ABC1(−496)* and *SID3(−431)*. (C) GEMSA result with the region of the *SID1* promoter that contains the GATA consensus (in bold, with the GATA elements underlined). The *SID1(−684)** probe consists of the 5′- and 3′-flanking sequences of the *SID1* GATA consensus fused together. The *SID1(−684)*** probe represents the GATA consensus of the *SID1(−684)* probe. The black arrow indicates the unbound probe, and the white arrows indicate the shifted species.

Table 2: Metal Stoichiometry of Purified Protein

construct	mutations	number of metals/monomer[a] iron	zinc
wild type		0.46 ± 0.02	1.60 ± 0.36
crr1	C219A/C225A	0.18 ± 0.07	1.33 ± 0.16
crr2	C234A/C237A	0.12 ± 0.01	1.25 ± 0.14
crr1−crr2	C219A/C225A/C234A/C237A	0.06 ± 0.02	1.35 ± 0.41
gzf1	C128A/C131A	0.24 ± 0.06	0.70 ± 0.12
gzf2	C291A/C294A	0.19 ± 0.12	0.94 ± 0.27
gzf1−gzf2	C128A/C131A/C291A/C294A	0.34 ± 0.11	0.60 ± 0.20

[a] The error was the standard deviations of triplicate determinations of the protein and metal concentrations.

Similar to the CRR mutants, the zinc finger mutants, gzf1 and gzf2, also contained less iron in comparison to wild-type Sre1p. Mutations in either zinc finger domain resulted in about half an equivalent less iron, whereas mutations in both domains appeared to partially compensate (~0.34 equiv).

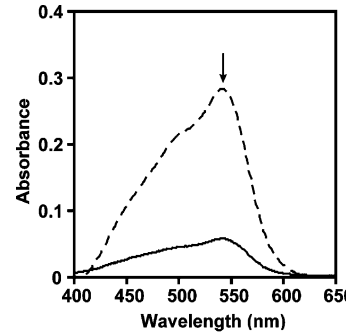

FIGURE 5: Iron content of purified Sre1p. Absorption spectrum of wild-type Sre1p bound to BPS with (• • •) or without (—) dithionite. The arrow identifies the BPS−Fe^{2+} peak at 540 nm.

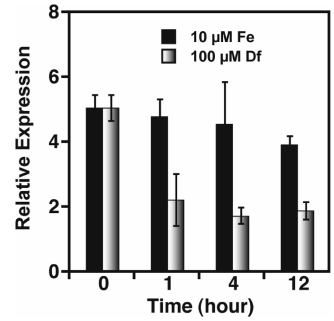

FIGURE 6: Effect of iron on *SRE1* expression. *SRE1* transcript levels relative to *ACT1* transcript levels were determined by qRT-PCR. RNA was isolated from cultures grown in HMM with 10 μM ferric citrate or 100 μM deferoxamine mesylate. Aliquots (10 mL) for RNA isolation were taken at 0, 1, 4, and 12 h.

The oxidation state of the bound iron was determined using the specific Fe^{2+} chelator BPS. The Fe^{2+}−BPS complex can be monitored by absorption spectroscopy and has an absorbance max at 540 nm (*34*). A 540 nm peak was observed when the reductant dithionite, which can reduce Fe^{3+} to Fe^{2+}, was added to the protein, indicating that the iron bound to native Sre1p was mostly Fe^{3+} (Figure 5). The small amount of Fe^{2+} observed in the protein sample prior to the addition of dithionite may be due to the protein being purified under reducing conditions and the ability of Fe^{3+} to be photochemically reduced to Fe^{2+} (*36*). Interestingly, when dithionite-treated Sre1p was desalted before BPS addition, little or no iron was detected (data not shown), indicating that Fe^{2+} did not stay bound to the protein. Furthermore, metal-free Sre1p could not be reconstituted with Fe^{2+} under anaerobic conditions.

Analysis of SRE1 Expression and Regulation. SRE1 expression in the yeast form of *H. capsulatum* G217B was examined under iron-limiting and iron-replete growth conditions. Quantitative PCR analysis indicated that *SRE1* was constitutively expressed in high-iron medium, whereas expression was reduced approximately ~2.5-fold when an iron chelator, such as deferoxamine, was added to the growth medium (Figure 6). This result differed from most other fungal GATA iron-mediated transcriptional regulators, which are constitutively expressed, with the exception of *A. nidulans sreA*, which is repressed under low iron-growth conditions and elevated under high iron-growth conditions (*23*).

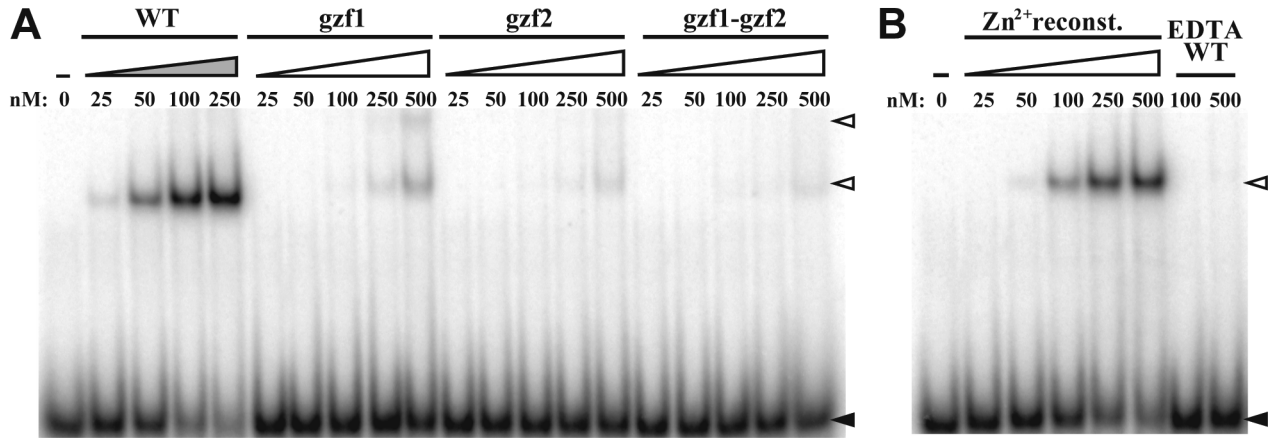

FIGURE 7: Zinc finger domains of Sre1p and DNA binding. (A) GEMSA comparing the wild type (WT) and the zinc finger mutants, gzf1 (C128A/C131A), gzf2 (C291A/C294A), and gzf1−gzf2 (C128A/C131A/C291A/C294A) using the ^{32}P-labeled *SID3(−575)* probe. (B) Comparison of EDTA-treated and Zn^{2+}-reconstituted Sre1p. The black arrow indicates the unbound probe, and the white arrows indicate the shifted species.

Zinc Dependence on DNA Binding by Sre1p. To examine the functional significance of the zinc finger domains, at least two of the four critical cysteines in each domain were replaced with alanines by site-directed mutagenesis, and the ability of the mutant proteins to bind DNA was assessed using the *SID3(−575)* probe. In comparison to wild-type Sre1p, mutations in either one or both zinc fingers domains resulted in a significant decrease in Sre1p binding to the target DNA (Figure 7A). Two faint band shifts were observed at high protein concentrations (0.5 μM) of the N-terminal GATA zinc finger mutant, gzf1 (C128A/C131A). The ability to bind DNA was even more severely affected with the C-terminal GATA zinc finger mutant, gzf2 (C291A/C294A), and double GATA zinc finger mutant, gzf1−gzf2 (C128A/C131A/C291A/C294A). These results indicated that the C-terminal GATA zinc finger domain in Sre1 played an important role in DNA binding, as observed for other fungal iron regulators (*23, 28, 35, 37*).

The effect of zinc metal on DNA binding was also examined (Figure 7B). Wild-type Sre1 protein that was dialyzed against EDTA to remove any iron or zinc metal associated with the protein did not bind DNA. When approximately 2 equiv of Zn^{2+} (determined by ICP-AES) was added back into the protein by dialyzing the protein against excess Zn^{2+}, Sre1p was able to bind DNA but with lower affinity (an apparent K_d of 230 nM; Table 1).

Iron Dependence on DNA Binding. To determine whether iron directly affected the ability of Sre1p to bind DNA, Zn^{2+}-reconstituted Sre1p was incubated in the presence or absence of Fe^{3+} at 4 °C overnight and then its activity was assessed by GEMSA using the *SID3(−575)* probe. Zn^{2+}-reconstituted Sre1p that was incubated with 1 equiv of Fe^{3+} bound DNA with higher affinity (∼2-fold) compared to the no iron control sample (Figure 8A). At least 0.5−1 equiv of Fe^{3+} was necessary to recover DNA binding (Figure 8B). However, excess iron (10-fold) slightly inhibited DNA binding. Interestingly, Zn^{2+}-reconstituted Sre1p that was incubated at 4 °C overnight had lower DNA-binding affinity (∼1.7 fold) compared to freshly reconstituted protein, which suggested that not only was iron necessary for full DNA binding but that it was also important in maintaining the stability of the Zn^{2+}-reconstituted protein. DNA binding was not rescued when the CRR mutant, crr1−crr2, was incubated with 1 equiv of Fe^{3+} (data not shown), which underscored the significance of the cysteine residues in coordinating Fe^{3+}.

To further elucidate the role of the cysteines in DNA binding, GEMSA using the *SID3(−575)* probe was also carried out with the CRR mutants, crr1, crr2, and crr1−crr2, and their apparent K_d values were determined (Figure 8C and Table 1). The mutants retained the ability to bind DNA but with approximately 2−2.5-fold lower affinity than the wild-type protein (apparent K_d of 90 nM). The crr1, crr2, and crr1−crr2 proteins bound to the GATA sequence with apparent K_d values of 250, 205, and 227 nM, respectively. These binding affinities were similar to the binding affinity for the Zn^{2+}-reconstituted wild-type protein (apparent K_d of 230 nM), which had no bound iron. ICP-AES analysis revealed that the purified CRR mutants (crr1, crr2, and crr1−crr2) contained little or no iron (Table 2). Together, these results showed that iron had a direct effect on the DNA-binding ability of Sre1p.

DISCUSSION

In this study, we identified *SRE1*, which encoded a GATA factor similar to the fungal GATA factors that negatively regulate genes involved in iron uptake. Analysis of promoter sequences upstream of *Histoplasma* genes that are iron-regulated identified a potential consensus regulatory site, 5′-(G/A)ATC(T/A)GATAA-3′ (*42*). Some of these genes contain more than one of these sequences. Gel-shift analysis using purified recombinant Sre1p(116−374) and probes that contained the consensus sequence indicated that DNA binding was GATA-specific and dependent upon both zinc fingers for optimal binding. Mutations in either zinc finger domain led to a significant loss in DNA binding, with the C-terminal domain mutation having a more severe defect. Both single- and multiple-shifted species were observed depending upon the probe used. A single band shift was observed at lower protein concentrations and when using probes that contained only one GATA. A second shift was observed at higher protein concentrations, which was probably due to Sre1p−Sre1p dimer formation. The *SID1* probe that contained more than one GATA, yielded at least three mobility-shifted species. The presence of multiple-shifted species was probably due to protein bound to more than one

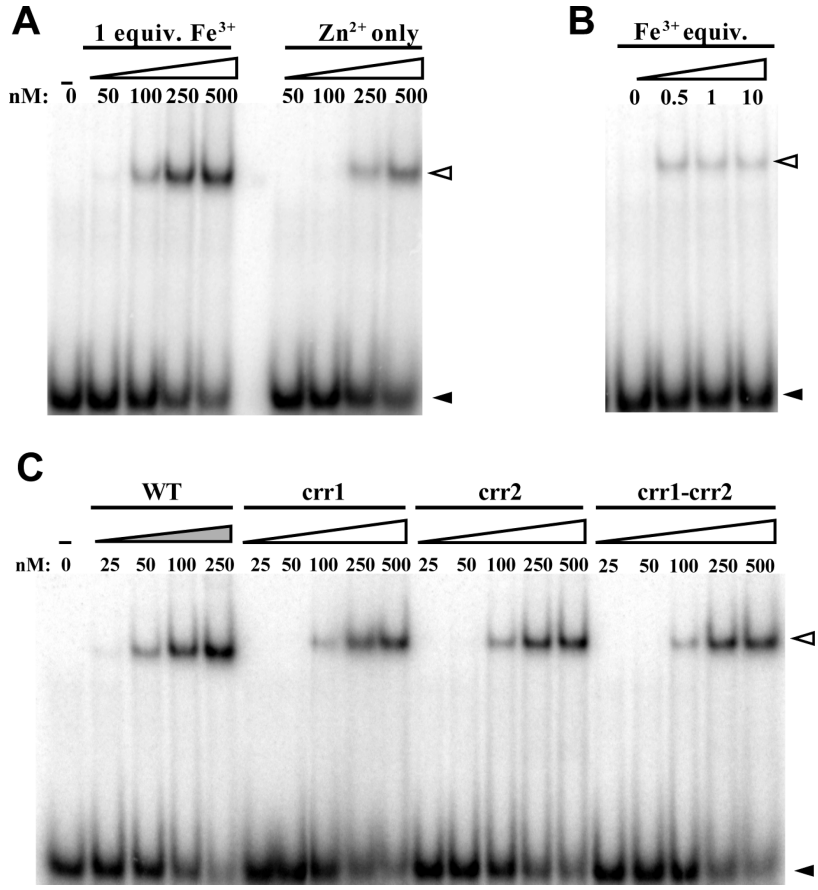

FIGURE 8: Effect of iron and the cysteine-rich region on Sre1p DNA binding. (A) GEMSA comparing Zn^{2+}-reconstituted Sre1p incubated in the presence of absence of Fe^{3+} using the *SID3(−575)* probe. An equamolar amount of ferric citrate was incubated with Zn^{2+}-reconstituted Sre1p overnight at 4 °C. A control sample of Zn^{2+}-reconstituted Sre1p without any ferric citrate was also included. (B) Zn^{2+}-reconstituted Sre1p was incubated in the presence of increasing amounts (0.5, 1, and 10 equiv) of ferric citrate for 25 min at room temperature before GEMSA using the *SID3(−575)* probe was performed. (C) CRR contributed to DNA-binding affinity. GEMSA using the *SID3(−575)* probe comparing the DNA-binding ability of wild-type Sre1p (WT) and the CRR mutants, crr1 (C219A/C225A), crr2 (C234A/C237A), and crr1−crr2 (C219A/C225A/C234A/C237A). The black arrow indicates the unbound probe, and the white arrows indicate the shifted species.

GATA site and/or Sre1−Sre1 dimer formation. Analytical gel filtration indicated that Sre1p(116−374) existed mainly as a monomer with a small percentage of dimer. Nevertheless, in vertebrate GATA factors, one of the zinc finger domains is involved in self-dimerization (*38, 39*), which may also be true for Sre1p (116−379).

A conserved 27 amino acid region with four highly conserved cysteines between the two zinc finger domains, common to the iron-regulatory fungal GATA factors, is involved in iron sensing *in vivo* (*26–28*). Unpublished tryptophan fluorescence experimental data suggested that there was an interaction between iron and *S. pombe* Fep1 [M. Durand, B. Pelletier, M. Bisaillon, and S. Labbé, unpublished data (*40*)]. However, whether these transcription factors sense iron by a reversible iron-binding event has not been directly tested. Here, we showed direct evidence for iron association with recombinant Sre1p(116−374) using ICP-AES. Metal analysis of purified protein indicated that iron binding was through the conserved cysteine residues in the CRR. Mutations of these conserved cysteine residues (crr1, C219 and C225A; crr2, C234 and C237A; and crr1−crr2, C219, C225, C234, and C237A) yielded protein with the least amount of bound iron. The GZF mutants also contained less iron, suggesting that the zinc finger domains may be involved in binding iron or stabilizing the protein when iron is bound.

In addition to determining the iron content of Sre1p, we found that the ferric oxidation state was predominantly bound to recombinantly expressed Sre1p. Although Fe^{2+} is thought to be the primary functional metal *in vivo*, there is evidence to suggest that Fe^{3+} can also activate other microbial iron-regulatory proteins (*41*). We only detected trace amounts of the Fe^{2+} bound to Sre1p, and the protein could not be reconstituted anaerobically with Fe^{2+}. Furthermore, the reduction of the protein-bound ferric form resulted in metal loss from Sre1p. Despite our observations, it is possible that other factors influence metal insertion and stability; hence, these observations do not preclude the possibility that both iron oxidation states are involved in Sre1 activity *in vivo*.

The zinc content of the purified wild-type and mutant proteins was also determined. The wild-type protein contained ∼2 equiv of zinc per monomer, which was consistent with there being two zinc finger domains. In contrast, the GZF mutants all contained less zinc, average ∼1 equiv of zinc per monomer. Interestingly, the double GZF mutant, gzf1−gzf2, still contained a small amount of zinc (0.6 equiv). This observation may reflect the fact that not all of the cysteine residues (4 of 8) predicted to ligate the zincs were mutated, and the remaining cysteines may still have bound a minimal amount of zinc. In addition, gel-mobility-shift analysis indicated that, although DNA binding was signifi-

cantly diminished in the zinc finger mutants, a small amount of protein still bound the specific DNA probe at higher protein concentrations, suggesting that the mutant protein still retained some of its structure. Mutations in the CRR also led to a slight decrease in bound zinc (~1.3 equiv), suggesting that iron and zinc binding were linked.

Although Zn^{2+} was necessary for DNA binding, iron (Fe^{3+}) also had a crucial role in the DNA-binding specificity. DNA binding of the Zn^{2+}-reconstituted Sre1p, which had a lower (~2.5 fold) apparent K_d similar to the CRR mutants, was rescued when 0.5−1 equiv of Fe^{3+} was present. At higher concentrations of Fe^{3+} (≥10-fold), DNA binding was inhibited. Furthermore, the Zn^{2+}-reconstituted protein lost its ability to bind DNA after prolonged exposure at 4 °C, indicating that Fe^{3+} was important for maintaining the DNA-binding activity *in vitro*. EDTA-treated wild-type Sre1p did not bind to target DNA, indicating that both zinc and iron were required for full activity.

qRT-PCR analysis also showed that *SRE1* was expressed under high-iron growth conditions, but its expression was repressed under iron-starving conditions, similar to the expression of the orthologue *SREA* in *A. nidulans* (*23*). In contrast, *N. crassa SRE*, *U. maydis URBS1*, and *S. pombe fep1*$^+$ are constitutively expressed (*24, 25, 29*).

Thus, relief of repression by Sre1p in iron-limiting conditions would appear to be accomplished by a 2.5-fold decrease in abundance based on SRE1 mRNA levels and a 2.5-fold decrease in affinity for the GATA motifs. At least 0.5−1 equiv of iron per Sre1p was necessary for full DNA-binding activity. It should be noted that the binding studies were performed on a fragment of protein lacking such features as the conserved C-terminal coiled-coil domain, and hence, its *in vitro* quantitative behavior may have underestimated the magnitude of its *in vivo* effects.

In summary, Sre1p was an iron-binding GATA-site-specific DNA-binding protein of iron-responsive genes in the fungal pathogen in *H. capsulatum*. Sre1p bound to the consensus sequence 5′-(G/A)ATC(T/A)GATAA-3′ in a manner mutually dependent upon both zinc and iron for highest affinity binding. Iron was directly associated with the protein and enhanced its DNA-binding affinity to target DNA. Iron was also important for the overall stability of the protein, making Sre1 a unique type of GATA factor that requires both zinc and iron for its full function. Interestingly, although expression of *SRE1* was iron-responsive, no GATA consensus was present in its promoter region, suggesting the possibility of another iron-regulated transcription factor present in *H. capsulatum*. Thus, iron homeostasis in *H. capsulatum* was probably regulated on several levels to maintain the appropriate levels of essential iron within the cell.

ACKNOWLEDGMENT

We thank Hans Carlson, Emily Weinert, Rosalie Tran, Anita Sil, and Lena Hwang for critical reading of this manuscript. We also thank Stephen Mills and members of the Marletta, Rine, and Sil labs for useful discussion. We are especially grateful to Jacquin Niles for help and inspiration throughout this project.

SUPPORTING INFORMATION AVAILABLE

One table showing the complete nucleotide sequences of the probes used for the GEMSAs. This material is available free of charge via the Internet at http://pubs.acs.org.

REFERENCES

1. Retallack, D. M., and Woods, J. P. (1999) Molecular epidemiology, pathogenesis, and genetics of the dimorphic fungus *Histoplasma capsulatum*. *Microbes Infect. 1*, 817–825.
2. Guerinot, M. L. (1994) Microbial iron transport. *Annu. Rev. Microbiol. 48*, 743–772.
3. Lane, T. E., Wu-Hsieh, B. A., and Howard, D. H. (1991) Iron limitation and the γ interferon-mediated antihistoplasma state of murine macrophages. *Infect. Immun. 59*, 2274–2278.
4. Newman, S. L., Gootee, L., Brunner, G., and Deepe, G. S., Jr. (1994) Chloroquine induces human macrophage killing of *Histoplasma capsulatum* by limiting the availability of intracellular iron and is therapeutic in a murine model of histoplasmosis. *J. Clin. Invest. 93*, 1422–1429.
5. Newman, S. L., Gootee, L., Stroobant, V., van der Goot, H., and Boelaert, J. R. (1995) Inhibition of growth of *Histoplasma capsulatum* yeast cells in human macrophages by the iron chelator VUF 8514 and comparison of VUF 8514 with deferoxamine. *Antimicrob. Agents Chemother. 39*, 1824–1829.
6. Jurado, R. L. (1997) Iron, infections, and anemia of inflammation. *Clin. Infect. Dis. 25*, 888–895.
7. Timmerman, M. M., and Woods, J. P. (2001) Potential role for extracellular glutathione-dependent ferric reductase in utilization of environmental and host ferric compounds by *Histoplasma capsulatum*. *Infect. Immun. 69*, 7671–7678.
8. Wilks, A., and Burkhard, K. A. (2007) Heme and virulence: How bacterial pathogens regulate, transport and utilize heme. *Nat. Prod. Rep. 24*, 511–522.
9. Crichton, R. R. (2001) Solution chemistry of iron in biological media, in *Inorganic Biochemistry of Iron Metabolism: From Molecular Mechanisms to Clinical Consequences* pp 1−15, John Wiley and Sons, Ltd., New York.
10. Pierre, J. L., and Fontecave, M. (1999) Iron and activated oxygen species in biology: The basic chemistry. *BioMetals 12*, 195–199.
11. Litwin, C. M., and Calderwood, S. B. (1993) Role of iron in regulation of virulence genes. *Clin. Microbiol. Rev. 6*, 137–149.
12. Payne, S. M. (1993) Iron acquisition in microbial pathogenesis. *Trends Microbiol. 1*, 66–69.
13. Howard, D. H., Rafie, R., Tiwari, A., and Faull, K. F. (2000) Hydroxamate siderophores of *Histoplasma capsulatum*. *Infect. Immun. 68*, 2338–2343.
14. Renshaw, J. C., Robson, G. D., Trinci, A. P. J., Wiebe, M. G., Livens, F. R., Collison, D., and Taylor, R. J. (2002) Fungal siderophores: Structures, functions, and applications. *Mycol. Res. 106*, 1123–1142.
15. Crichton, R. R. (2001) Microbial iron uptake, in *Inorganic Biochemistry of Iron Metabolism: From Molecular Mechanisms to Clinical Consequences* pp 49−81, John Wiley and Sons, New York.
16. Neilands, J. B. (1995) Siderophores: Structure and function of microbial iron transport compounds. *J. Biol. Chem. 270*, 26723–26726.
17. Wandersman, C., and Delepelaire, P. (2004) Bacterial iron sources: From siderophores to hemophores. *Annu. Rev. Microbiol. 58*, 611–647.
18. Philpott, C. C. (2006) Iron uptake in fungi: A system for every source. *Biochim. Biophys. Acta 1763*, 636–645.
19. Marzluf, G. A. (1997) Genetic regulation of nitrogen metabolism in the fungi. *Microbiol. Mol. Biol. Rev. 61*, 17–32.
20. Orkin, S. H. (1992) GATA-binding transcription factors in hematopoietic cells. *Blood 80*, 575–581.
21. Scazzocchio, C. (2000) The fungal GATA factors. *Curr. Opin. Microbiol. 3*, 126–131.
22. Haas, H., Angermayr, K., and Stoffler, G. (1997) Molecular analysis of a *Penicillium chrysogenum* GATA factor encoding gene (sreP) exhibiting significant homology to the *Ustilago maydis* urbs1 gene. *Gene 184*, 33–37.
23. Haas, H., Zadra, I., Stoffler, G., and Angermayr, K. (1999) The *Aspergillus nidulans* GATA factor SREA is involved in regulation of siderophore biosynthesis and control of iron uptake. *J. Biol. Chem. 274*, 4613–4619.

24. Pelletier, B., Beaudoin, J., Mukai, Y., and Labbe, S. (2002) Fep1, an iron sensor regulating iron transporter gene expression in *Schizosaccharomyces pombe*. *J. Biol. Chem. 277*, 22950–22958.
25. Zhou, L. W., Haas, H., and Marzluf, G. A. (1998) Isolation and characterization of a new gene, sre, which encodes a GATA-type regulatory protein that controls iron transport in *Neurospora crassa*. *Mol. Gen. Genet. 259*, 532–540.
26. Harrison, K. A., and Marzluf, G. A. (2002) Characterization of DNA binding and the cysteine rich region of SRE, a GATA factor in *Neurospora crassa* involved in siderophore synthesis. *Biochemistry 41*, 15288–15295.
27. Mercier, A., Pelletier, B., and Labbe, S. (2006) A transcription factor cascade involving Fep1 and the CCAAT-binding factor Php4 regulates gene expression in response to iron deficiency in the fission yeast *Schizosaccharomyces pombe*. *Eukaryot. Cell 5*, 1866–1881.
28. Pelletier, B., Trott, A., Morano, K. A., and Labbe, S. (2005) Functional characterization of the iron-regulatory transcription factor Fep1 from *Schizosaccharomyces pombe*. *J. Biol. Chem. 280*, 25146–25161.
29. Voisard, C., Wang, J., McEvoy, J. L., Xu, P., and Leong, S. A. (1993) urbs1, a gene regulating siderophore biosynthesis in *Ustilago maydis*, encodes a protein similar to the erythroid transcription factor GATA-1. *Mol. Cell. Biol. 13*, 7091–7100.
30. Worsham, P. L., and Goldman, W. E. (1988) Quantitative plating of *Histoplasma capsulatum* without addition of conditioned medium or siderophores. *J. Med. Vet. Mycol. 26*, 137–143.
31. Pryor, K. D., and Leiting, B. (1997) High-level expression of soluble protein in *Escherichia coli* using a His6-tag and maltose-binding-protein double-affinity fusion system. *Protein Expression Purif. 10*, 309–319.
32. Christopolous, A., and Lew, M. J. (2001) Beyond eyeballing: Fitting models to experimental data, in *Biomedical Applications of Computer Modeling* (Christopolous, A., Ed.) pp 195−231, CRC Press, New York.
33. Motulsky, H. J., and Christopolous, A. (2003) Fitting dose−response curves, in *Fitting Models to Biological Data Using Linear and Nonlinear Regression. A Practical Guide to Curve Fitting*, pp 256−295, GraphPad Software, Inc., San Diego, CA.
34. Cowart, R. E., Singleton, F. L., and Hind, J. S. (1993) A comparison of bathophenanthrolinedisulfonic acid and ferrozine as chelators of iron(II) in reduction reactions. *Anal. Biochem. 211*, 151–155.
35. Zhou, L., and Marzluf, G. A. (1999) Functional analysis of the two zinc fingers of SRE, a GATA-type factor that negatively regulates siderophore synthesis in *Neurospora crassa*. *Biochemistry 38*, 4335–4341.
36. Mueller, S., and Simpson, R. J. (1994) Photoreduction of iron at physiological pH: Effect of biological buffers. *Biochem. Soc. Trans. 22*, 93S.
37. An, Z., Zhao, Q., McEvoy, J., Yuan, W. M., Markley, J. L., and Leong, S. A. (1997) The second finger of Urbs1 is required for iron-mediated repression of sid1 in *Ustilago maydis*. *Proc. Natl. Acad. Sci. U.S.A. 94*, 5882–5887.
38. Crossley, M., Merika, M., and Orkin, S. H. (1995) Self-association of the erythroid transcription factor GATA-1 mediated by its zinc finger domains. *Mol. Cell. Biol. 15*, 2448–2456.
39. Merika, M., and Orkin, S. H. (1995) Functional synergy and physical interactions of the erythroid transcription factor GATA-1 with the Kruppel family proteins Sp1 and EKLF. *Mol. Cell. Biol. 15*, 2437–2447.
40. Labbe, S., Pelletier, B., and Mercier, A. (2007) Iron homeostasis in the fission yeast *Schizosaccharomyces pombe*. *BioMetals 20*, 523–537.
41. Mills, S. A., and Marletta, M. A. (2005) Metal binding characteristics and role of iron oxidation in the ferric uptake regulator from *Escherichia coli*. *Biochemistry 44*, 13553–13559.
42. Hwang, L. H., Mayfield, J. A., Rine, J., and Sil, A. (2008) Histoplasma requires SID1, a member of an iron-regulated siderophore gene cluster, For host colonization. *PLo S Pathog. 4*, e1000044.

BI800066S